THE ASTROPHYSICAL JOURNAL, 289:247–261, 1985 February 1

EVOLUTION OF LOW-MASS STARS IN THE ALPHA PERSEI CLUSTER[1]

JOHN R. STAUFFER,[2] LEE W. HARTMANN, AND J. NEAL BURNHAM
Harvard-Smithsonian Center for Astrophysics

AND

BURTON F. JONES
Lick Observatory
Received 1984 June 25; accepted 1984 August 22

ABSTRACT

We present a photometric and spectroscopic study of low-mass members of the α Persei cluster. New relative proper motions have been obtained for 4000 stars in a 1°.2 × 1°.2 region of the α Persei open cluster. The survey extends to $V \approx 16.5$ mag, much fainter than the previous proper motion surveys. Optical photometry and high-dispersion spectroscopy of the possible cluster members from our survey, as well as a set of 10th to 12th magnitude stars from previous surveys, have also been obtained. The new photometry shows an apparent pre–main sequence (PMS), but we cannot yet accurately determine the PMS turn-on point. The faint stars in the cluster have positions in a V versus $V-I$ diagram that are roughly in accord with the 5×10^7 yr isochrone derived by VandenBerg *et al.*

In agreement with previous results for the Pleiades cluster, some of the late-type α Persei members are photometric variables, with periods of 1 day or less. Light curves and estimated periods are presented for six of the G and K dwarf members of the cluster. We attribute the periodic light variations to spots on the surfaces of these stars, which are carried around the visible hemisphere by rapid rotation. The photometric periods are consistent with rotational broadening measurements when available.

Projected rotational velocities derived from the echelle spectra indicate that nearly 50% of the stars observed that are later than G2 have 25 km s^{-1} < $v \sin i$ < 150 km s^{-1}. The large rotational velocities among low-mass stars in young clusters are ascribed to spin-up during contraction to the main sequence. Since K dwarfs in the Hyades cluster do not show such anomalous rotational velocities, the spin-down time to $v \sin i$ < 10 km s^{-1} must be on the order of or less than a few hundred million years. Comparison with the rotational velocity data derived for stars in the Pleiades indicates that the spin-down time for G dwarfs must be much shorter, less than 2–3 × 10^7 yr.

Subject headings: clusters: open — stars: evolution — stars: pre–main-sequence — stars: proper motion — stars: rotation

I. INTRODUCTION

In the last few years, our picture of the evolution of rotation among low-mass stars has changed dramatically. Early studies (cf. Kraft 1967*b*) indicated that stars with masses less than about 1.2 $M_{\odot}$ generally rotate at less than 20 km s^{-1}, and this has been confirmed in more detail by subsequent observations (Vaughan *et al.* 1981; Soderblom 1983; and references therein). However, it has now become clear that there are very rapidly rotating, main-sequence K dwarfs in the Pleiades cluster (van Leeuwen and Alphenaar 1982; Soderblom, Jones, and Walker 1983; Stauffer *et al.* 1984, hereafter SHSB). In our recent paper (SHSB), we showed that a significant fraction of the Pleiades dwarfs with spectral types later than K2 are rapid rotators, with 30 < $v \sin i$ < 150 km s^{-1}. This is to be contrasted with the G dwarfs, which show rotational velocities $v \sin i$ < 30 km s^{-1}. The spectroscopic and photometric measurements show that the rapid rotators are not members of close binaries, nor are they at a significantly different evolutionary stage than the slow rotators.

Our interpretation of these data is that the decrease in stellar moment of inertia during contraction to the main sequence causes low-mass stars to spin up considerably. The G dwarfs in the Pleiades reached the main sequence approximately 4 × 10^7 yr ago, so that magnetic braking via a stellar wind has had time to spin down the star. The K dwarfs have just reached the main sequence, so that they still spin rapidly. It may also be that only the thin convective envelope of a G dwarf is spun down at first (cf. Endal and Sofia 1981), increasing the difference in surface rotation between the Pleiades G and K stars.

This scenario predicts that a somewhat younger cluster will have rapidly rotating G stars. To test this idea, we have examined the α Persei cluster (age ≈ 5 × 10^7 yr, Mermilliod 1981). This has required a new proper motion survey in order to identify the low-mass members of this cluster. Previous proper motion measurements of the α Persei cluster have been obtained by Heckmann, Dieckvoss, and Kox (1956, hereafter HDK), Artyukhina (1972), and Fresneau (1980). Those authors find that the cluster contains approximately 150 members brighter than $B \approx 12$ mag (the approximate magnitude limit of those surveys), and that most of the cluster members are located in a core region with radius r = 1°.25. Photometry of the HDK sample has been reported by Mitchell (1960) and Crawford and Barnes (1974); rotational velocities for many of those stars have been estimated by Abt and Hunter (1962) and

[1] Research reported here was accomplished using the Multiple Mirror Telescope Observatory, a joint facility of the Smithsonian Institution and the University of Arizona.

[2] Visiting Astronomer, Kitt Peak National Observatory, which is operated by the Association of Universities for Research in Astronomy, Inc., under contract with the National Science Foundation.

TABLE 1

PLATE DATA

Number	Epoch	Exposure	Emulsion	Filter	Telescope
E1249	1954.76	40 min	103a-E	red Plexiglas	Schmidt
O1249	1954.76	10 min	103a-O	...	Schmidt
PS28128	1981.06	10 min	103a-D	...	Schmidt
PS28129	1981.06	40 min	103a-D	WR25	Schmidt
AB1379	1949.75	2 hr	103a-O	...	Astrograph
AB9168	1981.91	2 hr	103a-O	...	Astrograph
AY9168	1981.91	2 hr	103a-G	GG13	Astrograph

Kraft (1967*a*). These surveys do not extend to faint enough stars to test the hypothesis of rapid evolution of rotation in G dwarfs. In this paper, we present proper motions, photometry, and spectroscopy for faint stars in the α Persei cluster.

Our own proper motion survey covers only the central portion of the cluster, but extends to $V \approx 17$ mag, with a bright limit corresponding roughly to the faint limit of the previous surveys. In § II, we describe the details of our new proper motion survey of the cluster. New photometry of those stars, as well as the fainter stars in the HDK sample, is reported in § III. Rotational and radial velocities for a subset of the stars for which photometry was obtained are presented in § IV. The final section provides a discussion of the implications of the new α Persei data, including a more complete description of our model to explain the angular momentum evolution of young, low-mass stars.

II. PROPER MOTIONS

Proper motion membership discrimination for the α Per cluster is more difficult than for other nearby clusters. This is because the motion of the cluster is small and in nearly the same direction as the reflex solar motion, and because the cluster is projected against a rich Milky Way background. However, we believed that with the available plate material, the proper motion errors would be small enough so that we could eliminate at least the majority of field stars from consideration and compile a small list of probable members. This proved to be the case.

We had available for measurement the glass copies of the Palomar–National Geographic Society Sky Survey and two second-epoch plates obtained in 1981, all taken with the Palomar 48 inch (1.2 m) Schmidt (scale 67″ mm^{-1}), and three plates taken for the Lick Proper Motion Program with the twin Carnegie 20 inch (51 cm) astrograph (scale 55″ mm^{-1}). The plate details are given in Table 1. The plates were measured on the Lick Automatic Measuring Engine.

Nearly 4,000 stars were surveyed in a region of 1.6 deg^2 near the cluster center, to a limiting magnitude of $V \sim 17$. These 4,000 stars were measured on all the Schmidt plates. Because of software limitations, we could only measure 1,000 stars at a time. Forty stars uniformly spread over the measuring area tied all the measures of a single plate onto a uniform system. These Schmidt measures were reduced for proper motion using a modified central overlap technique (Herbig and Jones 1981). All stars of small proper motion were used for the reference frame, and thus the proper motions are relative to the mean motion of the stars in the frame. We have made no attempt to reduce the motions to an absolute frame since our main purpose was to pick out α Per members. Considering the magnitude range of our reference frame stars, the correction would be quite small in any case—on the order of 0″.3 per century in each coordinate (van Altena 1974).

Figure 1 is a proper motion vector diagram of all stars measured with proper motions in x between $-2''$ and $5''$ per century and in y between $-4''$ and $2''$ per century. Note that there is little concentration of points at the expected motion for α Per members ($\mu_x = +2''.5$ per century, $\mu_y = -2''.0$ per century), shown as a large cross in Figure 1. If only the brighter half of our magnitude range is plotted, the cluster becomes more evident; the faint end of our sample shows no concentration at all. Because of the small number of possible α Per members, we did not make a standard proper motion membership analysis, but rather picked all stars with motions that were consistent with membership for further study, a total of 88 stars. The possible members that were bright enough were then measured on the astrograph plates, along with a selection of AGK3 stars used as a positional reference frame. The astrograph measures were reduced for proper motion in a manner similar to the Schmidt measures. Because the reference frame used for this reduction was different from the proper motions determined from the Schmidt measures, there was a large zero difference between the two sets of proper motions. The proper motions determined from the astrograph measures were corrected for this zero-point difference, and the two sets of motions were then averaged, giving each set equal weight. A comparison of the two sets of motions gives an error of 0″.9 per

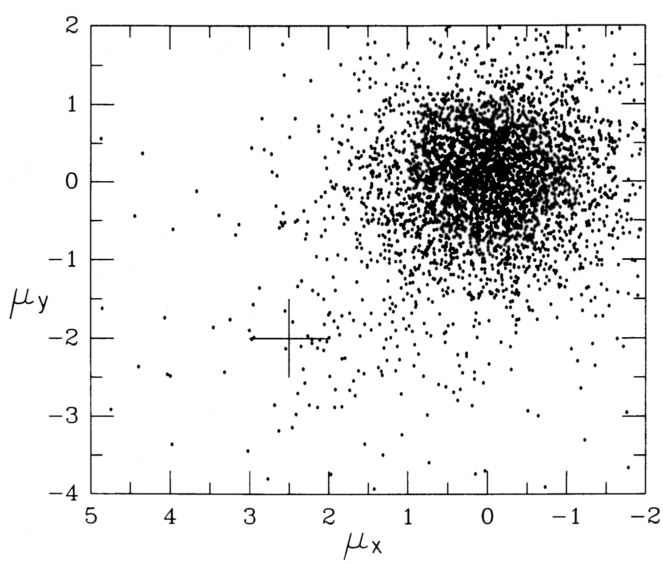

FIG. 1.—Proper motion diagram for stars toward the center of the α Persei cluster. The coordinate axes are μ_x and μ_y in arcsec per century. The large cross denotes the expected motion for true members of the cluster.

1985ApJ...289..247S

TABLE 2

NEW MEMBERS OF ALPHA PERSEI

AP	α	δ	μ_x (σ)	μ_y (σ)	V	Wt.
1......	$3^h19^m33\overset{s}{.}52$	49°06′49″.24	1.7 (0.4)	−1.6 (0.7)	14.87	2
2......	3 19 33.58	48 22 16.07	1.9 (0.3)	−1.4 (0.2)	15.6	1
3......	3 19 34.98	48 31 51.99	3.1 (1.2)	−1.3 (0.3)	15.54	2
4......	3 19 37.56	48 43 16.21	2.2 (0.5)	−2.8 (0.2)	16.09	2
5......	3 19 45.36	48 10 59.18	21. (0.5)	−1.5 (1.5)	16.1	1
6......	3 20 09.30	48 59 54.42	2.6 (0.7)	−1.6 (0.3)	15.39	2
7......	3 20 33.99	48 29 04.09	3.8 (0.6)	−1.4 (0.4)	16.06	2
8......	3 20 34.35	48 00 35.33	0.3 (0.2)	−1.0 (0.7)	16.0	2
9......	3 20 36.24	48 31 09.54	0.9 (1.1)	−1.1 (0.5)	13.48	2
10......	3 20 36.71	48 13 21.47	3.0 (0.3)	−1.9 (0.3)	12.10	1
11......	3 20 40.04	48 59 32.66	1.1 (0.4)	−0.9 (1.0)	13.66	2
12......	3 20 40.16	48 54 36.71	4.0 (1.0)	−2.1 (0.9)	14.96	2
13......	3 20 45.70	49 02 41.43	1.5 (0.4)	−1.7 (0.5)	10.1	1 He 606
14......	3 20 47.34	48 36 44.92	1.8 (0.3)	−2.3 (0.0)	11.94	1
15......	3 20 52.48	48 37 46.76	2.5 (0.8)	−2.3 (0.3)	14.12	2
16......	3 20 53.63	48 33 32.86	2.3 (0.3)	−1.3 (0.4)	15.5	1
17......	3 20 58.47	49 07 53.82	2.4 (0.3)	−2.3 (0.7)	15.27	2
18......	3 21 07.95	49 05 20.90	3.0 (0.1)	−3.4 (0.2)	16.2	1
19......	3 21 16.85	48 41 45.44	1.4 (0.1)	−2.4 (0.3)	11.62	1
20......	3 21 19.22	48 53 41.80	2.4 (0.7)	−2.2 (0.3)	15.66	2
21......	3 21 28.13	48 51 33.27	3.3 (0.0)	−1.8 (0.4)	15.56	2
22......	3 21 34.44	48 38 54.15	2.1 (0.3)	−1.4 (1.1)	16.2	1
23......	3 21 39.32	48 20 12.40	1.6 (0.7)	−1.3 (0.5)	16.2	1
24......	3 21 41.04	48 28 17.05	2.2 (0.2)	−1.0 (0.3)	16.3	1
25......	3 21 44.31	48 11 52.28	1.8 (0.3)	−2.9 (0.4)	12.25	1
26......	3 21 46.09	48 55 48.94	1.8 (1.1)	−3.0 (0.6)	15.7	2
27......	3 22 19.11	48 26 16.98	0.1 (0.9)	−0.7 (1.1)	16.46	2
28......	3 22 51.59	48 20 39.39	1.6 (1.0)	−2.4 (0.5)	13.09	2
29......	3 22 26.25	48 27 22.42	1.8 (0.3)	−0.9 (0.2)	15.93	2
30......	3 22 27.98	48 31 26.65	1.7 (0.5)	−2.6 (1.3)	12.31	2
31......	3 22 28.78	48 54 09.53	1.0 (0.4)	−1.7 (0.4)	14.5	2
32......	3 22 31.26	48 37 37.95	1.7 (0.2)	−2.5 (0.2)	10.59	2 He 684
33......	3 22 41.00	47 58 40.46	1.8 (0.6)	−2.5 (0.1)	12.94	2
34......	3 22 41.38	48 32 09.64	1.5 (0.6)	−3.3 (0.1)	15.8	1
35......	3 22 42.13	49 02 17.53	1.5 (0.4)	−1.1 (0.2)	15.9	1
36......	3 22 42.98	48 14 46.83	3.5 (0.1)	−2.6 (1.0)	14.23	2
37......	3 22 43.32	48 40 00.24	2.1 (0.7)	−2.5 (0.5)	12.61	2
38......	3 22 45.42	49 03 04.01	2.7 (0.4)	−2.0 (0.7)	11.61	2 He 696
39......	3 22 50.21	48 16 32.95	1.4 (0.7)	−1.8 (0.5)	16.4	1
40......	3 22 52.03	48 56 48.32	2.9 (1.1)	−1.4 (0.3)	15.8	1
41......	3 22 53.27	48 09 39.21	2.5 (0.7)	−1.7 (0.3)	12.03	2
43......	3 22 54.12	48 51 44.79	2.1 (0.5)	−2.6 (0.3)	12.84	2
44......	3 22 56.56	48 15 16.06	1.5 (1.0)	−0.9 (0.3)	16.6	1
45......	3 22 57.50	48 31 53.65	0.8 (0.3)	−1.6 (0.4)	15.20	2
46......	3 23 00.18	48 59 17.94	2.0 (0.4)	−0.8 (0.2)	13.4	2
47......	3 23 04.12	48 48 43.43	1.7 (0.2)	−1.4 (0.2)	14.1	2
48......	3 23 06.84	49 06 33.79	1.7 (0.7)	−1.8 (0.5)	14.83	2
49......	3 23 07.72	48 36 09.84	1.8 (0.1)	−1.7 (0.5)	9.75	1 He 715
50......	3 23 08.84	48 50 07.25	1.0 (1.2)	−2.0 (0.2)	11.4	2
51......	3 23 17.02	48 37 05.60	1.8 (0.3)	−2.3 (0.2)	10.32	1 He 727
52......	3 23 19.36	48 51 10.28	1.9 (0.5)	−1.7 (0.1)	14.9	2
53......	3 23 20.05	48 33 24.95	0.7 (0.4)	−1.7 (0.6)	15.48	2
54......	3 23 25.22	48 51 55.60	1.3 (0.6)	−3.5 (1.1)	13.7	1
55......	3 23 39.12	47 58 36.67	2.1 (0.4)	−1.9 (0.5)	13.91	2
56......	3 23 50.99	48 12 00.06	2.0 (0.1)	−2.6 (0.1)	13.00	2
57......	3 23 56.70	48 41 46.96	2.6 (0.6)	−3.2 (0.9)	15.7	1
58......	3 24 04.11	48 49 04.99	1.7 (0.3)	−2.7 (0.4)	10.57	1 He 750
59......	3 24 05.53	49 06 37.20	2.2 (0.3)	−2.6 (1.3)	14.85	2
60......	3 24 06.14	48 14 35.57	2.1 (0.7)	−3.0 (0.4)	15.82	2
61......	3 24 14.03	48 49 55.50	1.0 (0.3)	−2.1 (0.1)	13.5	2
62......	3 24 14.60	48 45 02.11	3.7 (0.6)	−0.8 (0.5)	16.3	2
63......	3 24 16.83	49 01 47.00	2.3 (0.1)	−0.5 (0.5)	12.9	2
64......	3 24 24.31	49 09 16.37	1.4 (0.3)	−2.6 (1.2)	15.5	2
65......	3 24 27.03	48 49 38.87	1.4 (0.1)	−2.8 (0.8)	13.5	2
66......	3 24 32.48	48 52 43.96	2.5 (0.7)	−1.6 (0.4)	12.1	1
67......	3 24 35.60	49 14 39.64	3.5 (0.5)	−1.9 (0.7)	16.5	1
68......	3 24 39.30	49 02 51.78	4.0 (0.2)	−3.3 (0.3)	14.2	2
69......	3 24 43.01	48 13 50.10	1.6 (0.6)	−0.8 (0.3)	16.15	2
70......	3 24 45.56	48 29 26.92	2.0 (0.2)	−1.8 (0.4)	12.83	2
71......	3 24 45.68	48 51 05.25	1.8 (0.6)	−1.8 (0.6)	14.1	2
72......	3 24 48.15	49 04 08.25	1.9 (0.5)	−2.0 (0.3)	13.6	2

TABLE 2—*Continued*

AP	α	δ	μ_x (σ)	μ_y (σ)	V	Wt.
73......	3 24 50.76	48 43 24.81	3.3 (0.4)	−2.4 (0.9)	12.05	1
74......	3 25 01.06	48 23 35.31	3.2 (0.7)	−1.1 (0.3)	16.08	2
75......	3 25 12.88	49 06 08.39	2.4 (0.8)	−2.9 (0.5)	14.2	2
76......	3 25 16.22	48 10 05.17	2.5 (0.7)	−3.1 (1.0)	16.4	1
77......	3 25 17.10	49 08 10.96	1.9 (0.8)	−0.7 (0.2)	16.1	2
78......	3 25 51.83	49 10 17.85	2.0 (0.5)	−2.5 (0.1)	13.06	2
79......	3 25 53.85	48 01 54.17	2.1 (0.1)	−2.2 (0.8)	10.00	1 He 848
80......	3 26 02.92	49 11 40.60	1.2 (0.4)	−1.4 (0.5)	15.00	2
81......	3 26 07.29	49 08 59.92	2.5 (0.3)	−2.0 (0.4)	12.43	2
82......	3 26 12.26	48 05 08.79	3.0 (0.1)	−2.7 (0.2)	12.73	2
83......	3 26 12.68	48 50 17.76	2.1 (0.9)	−2.0 (0.7)	9.21	1 He 863
84......	3 26 25.99	49 07 28.31	1.9 (0.1)	−2.0 (1.1)	16.2	1
85......	3 26 47.89	48 47 03.88	2.3 (0.8)	−2.4 (1.1)	16.08	2
86......	3 26 49.51	48 14 27.02	2.5 (0.9)	−2.4 (0.0)	14.31	2
87......	3 27 06.39	49 03 56.36	1.4 (0.5)	−0.7 (0.5)	15.91	2
88......	3 27 14.71	48 07 11.19	0.8 (0.6)	−1.3 (0.7)	14.01	2

century in μ_x and 0".7 per century in μ_y for proper motion measured on both sets of plates.

The AGK3 stars measured on the astrograph plates were used to set up a secondary reference frame. This secondary reference frame was then used to derive positions for all of the possible members. Also given in Table 2 is the magnitude of the star, photoelectrically determined if two decimal digits are given, or estimated from the photometry of the Schmidt plates (accuracy 0.5 mag) if only one decimal digit is given. The last column gives the weight, with weight 1 for proper motions determined from Schmidt measures only, and weight 2 for proper motions determined on both Schmidt and astrograph plates.

III. OPTICAL PHOTOMETRY

The optical photometry reported here was obtained during two nights on the #2 0.9 m telescope and five nights on the 1.3 m telescope at Kitt Peak, using the automated filter photometer (AFP) and the Mk II computer-controlled photometer, respectively. The standard Kitt Peak *BVRI* filter set was used with both photometers. Instrumental magnitudes were converted to Johnson V and $(B-V)$ values and Kron $(V-R)$ and $(R-I)$ colors via the same techniques employed for the open cluster photometry reported by us in previous papers (Stauffer 1984, and references therein). A list of the standard stars observed can be found in Stauffer (1982).

Table 3 provides a list of the new optical photometry obtained for stars in the α Per cluster. Except for the faintest stars ($V > 16$ mag), the colors and magnitudes are believed to have 1 sigma accuracies of about 0.015 mag. The $(B-V)$ colors for a few stars may have larger errors due to B band background gradients produced by scattered light from the many bright, nearby stars. We attempted to minimize that problem through judicious choice of the location of the sky aperture, but for some stars even the best location showed contamination. A quantitative estimate of the photometric errors for the brighter α Per stars observed can be made by comparison with the *UBV* photometry obtained by Mitchell (1960). Excluding three stars with quite large differences relative to Mitchell's photometry (He 656, He 696, and He 917), the mean differences between the present photometry and Mitchell's are $\langle \Delta V \rangle = 0.025$ (50 stars) with a dispersion of 0.028 mag, and $\langle \Delta(B-V) = 0.002$ with a dispersion of 0.021 mag. No previous photometry exists for the fainter stars in our sample, and intercomparison of multiple observations of those stars does not provide an indication of the errors in the photometry since we believe many of those stars are photometric variables.

Figure 2 shows a color-magnitude diagram for all of the stars observed for this program. A moderately well defined cluster main sequence is evident in the figure, but it is also clear that many of the stars observed have photometric properties inconsistent with membership in the cluster. A color-magnitude diagram for only probable cluster members will be presented in § V.

A number of the late-type α Per stars were observed repeatedly in order to search for photometric variability. The stars were selected on the basis of their large $v \sin i$'s derived from echelle spectra reported in § IV. Based on the close correlation between large rotational velocity and the short-period, photometric variability noted for the late-type Pleiades stars, we expected many of these α Per stars also to be photometric variables. The individual observations for those stars are given in Table 4. Examination of the entries in that table shows that many of the stars are indeed variable.

For each of the stars observed at least 10 times, the photometry was searched for periodicities. We used the modified periodogram method described by Scargle (1982), which is particularly suited to the analysis of unevenly sampled data. The method was implemented in a software routine written by J. Horne. The program has been successfully used to derive photometric periods for late-type dwarfs in the Hyades (Lockwood *et al.* 1984).

In Figure 3*a* we show the modified periodogram for the V magnitude observations of AP 56. The strongest peak corresponds to an 8.65 hr period. Subtraction of that frequency from the power spectrum leaves the residual power spectrum shown in Figure 3*b*. This subtraction removes the two subsidiary peaks in the periodogram, demonstrating that these peaks are not independent of the main peak, but are aliases of it. Using Scargle's (1982) results, we estimate that the "false alarm probability" for the 8.65 hr period is less than 2×10^{-4}. The light curve generated for AP 56 using this period is shown in Figure 4*d*.

Table 5 provides a list of periods derived in this manner for all of the stars for which we have sufficient photometric data. The rotational velocities in that table were derived assuming radii appropriate for their $V-I$ colors (only approximately correct since some of the stars are slightly above the main

TABLE 3

OPTICAL PHOTOMETRY

Name	V	$B-V$	$V-R$	$R-I$	$V-I$	N
He 326	12.15	0.58	0.23	0.28	0.51	1
He 330	9.89	1.31	0.66	0.52	1.18	1
He 334	10.37	0.55	0.21	0.24	0.45	1
He 350	11.13	0.71	0.34	0.31	0.65	1
He 407	11.18	0.64	0.27	0.25	0.52	1
He 444	11.16	0.83	0.39	0.36	0.75	1
He 453	10.41	0.61	0.27	0.26	0.53	1
He 457	11.72	0.73	0.36	0.32	0.68	1
He 462	11.49	0.83	0.41	0.35	0.76	1
He 477	10.60	1.47	0.74	0.54	1.28	1
He 481	9.18	0.36	0.10	0.13	0.23	1
He 490	9.59	0.43	0.14	0.17	0.31	2
He 493	11.05	0.57	0.24	0.25	0.49	1
He 501	9.18	0.33	0.06	0.11	0.17	1
He 520	11.69	0.79	0.37	0.32	0.69	25
He 537	10.15	1.16	0.55	0.45	1.00	1
He 538	11.61	0.66	0.33	0.32	0.65	1
He 551	11.20	0.65	0.29	0.27	0.56	1
He 574	8.96	1.27	0.60	0.45	1.05	1
He 588	10.01	0.54	0.23	0.25	0.48	1
He 595	10.38	0.51	0.19	0.21	0.40	1
He 600	11.90	0.68	0.32	0.29	0.61	1
He 601	11.43	0.73	0.32	0.27	0.59	1
He 608	11.19	0.60	0.27	0.27	0.54	1
He 609	9.23	0.42	0.14	0.17	0.31	1
He 632	9.73	0.46	0.16	0.18	0.34	1
He 647	10.35	0.42	0.13	0.17	0.30	1
He 656	11.85	0.52	0.20	0.23	0.43	1
He 660	10.10	0.57	0.24	0.26	0.50	1
He 676	11.43	0.65	0.28	0.27	0.55	1
He 680	9.69	1.46	0.71	0.52	1.23	1
He 699	11.27	0.71	0.32	0.29	0.61	1
He 707	10.05	0.77	0.33	0.31	0.64	1
He 709	10.95	0.68	0.30	0.29	0.59	2
He 721	9.66	0.51	0.19	0.23	0.42	2
He 732	10.21	0.55	0.21	0.22	0.43	1
He 767	10.69	0.62	0.25	0.26	0.51	1
He 771	11.14	0.68	0.33	0.33	0.66	1
He 794	10.09	0.54	0.22	0.24	0.46	1
He 815	11.19	1.44	0.70	0.54	1.24	1
He 841	10.29	0.54	0.21	0.23	0.44	1
He 859	10.52	0.56	0.23	0.25	0.48	1
He 879	10.41	0.47	0.18	0.21	0.39	1
He 917	10.93	0.66	0.29	0.28	0.57	1
He 935	10.05	0.62	0.26	0.26	0.52	1
He 936	11.40	0.61	0.27	0.27	0.54	1
He 979	11.66	0.56	0.26	0.27	0.53	1
AP 1	14.87	1.40	0.72	0.56	1.28	2
AP 3	15.54	1.05	0.54	0.35	0.78	1
AP 4	16.09	1.26	0.62	0.53	1.15	1
AP 6	15.39	1.56	1.07	0.90	1.97	2
AP 7	16.06	0.85	0.62	0.43	1.05	1
AP 9	13.48	0.80	0.43	0.38	0.81	1
AP 10	12.10	0.36	0.08	0.16	0.24	1
AP 11	13.66	0.74	0.35	0.33	0.68	1
AP 12	14.96	1.06	0.55	0.44	0.99	1
AP 14	11.94	0.83	0.37	0.32	0.69	2
AP 15	14.12	1.29	0.78	0.58	1.36	21
AP 17	15.27	1.55	1.07	0.91	1.98	2
AP 19	11.62	0.79	0.38	0.32	0.70	2
AP 20	15.66	1.55	1.28	1.07	2.35	2
AP 21	15.56	1.60	1.13	0.95	2.08	2
AP 25	12.25	0.88	0.41	0.34	0.75	1
AP 26	15.92	0.89	0.40	0.32	0.72	1
AP 27	16.46	1.14	0.57	0.55	1.12	1
AP 28	13.09	1.05	0.54	0.43	0.97	2
AP 29	15.93	1.27	0.62	0.49	1.11	1
AP 30	12.31	0.80	0.33	0.28	0.61	2
AP 31	14.35	0.83	0.37	0.32	0.69	1
AP 32	10.59	0.57	0.23	0.22	0.45	3
AP 33	12.94	1.04	0.52	0.37	0.89	1
AP 36	14.23	1.16	0.57	0.40	0.97	2
AP 37	12.61	0.96	0.47	0.38	0.85	2
AP 38	11.61	0.76	0.34	0.31	0.65	3
AP 41	12.03	0.85	0.38	0.33	0.71	1
AP 43	12.84	0.97	0.52	0.44	0.96	24
AP 45	15.20	0.92	0.48	0.38	0.86	2
AP 46	12.41	0.78	0.33	0.29	0.62	1
AP 47	13.69	0.87	0.40	0.36	0.76	1
AP 48	14.83	1.04	0.58	0.41	0.99	1
AP 49	9.75	0.48	0.16	0.18	0.34	3
AP 50	10.44	1.20	0.58	0.46	1.04	1
AP 51	10.32	0.56	0.22	0.24	0.46	3
AP 52	15.15	1.25	0.65	0.49	1.14	1
AP 53	15.48	1.11	0.54	0.44	0.98	1
AP 54	12.90	0.86	0.37	0.32	0.69	2
AP 55	13.91	1.11	0.56	0.41	0.97	1
AP 56	13.00	1.00	0.53	0.43	0.96	27
AP 58	10.59	0.59	0.23	0.23	0.46	2
AP 59	14.85	0.94	0.40	0.41	0.81	1
AP 60	15.82	1.70	1.34	1.13	2.47	3
AP 61	12.77	1.09	0.56	0.42	0.98	2
AP 62	16.84	1.43	0.65	0.53	1.18	1
AP 63	12.29	0.92	0.45	0.39	0.84	1
AP 65	13.00	1.05	0.52	0.39	0.91	2
AP 68	13.38	1.10	0.58	0.42	1.00	2
AP 69	16.15	1.13	0.57	0.41	0.98	1
AP 70	12.83	1.00	0.49	0.39	0.88	40
AP 71	13.46	0.76	0.38	0.32	0.70	1
AP 72	12.78	0.99	0.49	0.38	0.87	2
AP 73	12.05	0.68	0.30	0.28	0.58	2
AP 74	16.08	1.20	0.72	0.51	1.23	1
AP 75	13.82	1.27	0.79	0.63	1.42	2
AP 77	16.27	1.04	0.53	0.32	0.85	1
AP 78	13.06	1.02	0.53	0.43	0.96	2
AP 79	10.00	0.60	0.23	0.23	0.46	2
AP 80	15.00	0.87	0.44	0.38	0.82	2
AP 81	12.43	0.90	0.39	0.34	0.73	2
AP 82	12.73	0.88	0.41	0.35	0.76	1
AP 83	9.21	0.51	0.19	0.20	0.39	2
AP 85	16.08	1.39	0.77	0.53	1.30	1
AP 86	14.31	1.32	0.81	0.60	1.41	31
AP 87	15.91	1.02	0.48	0.48	0.96	1
AP 88	14.01	0.76	0.35	0.31	0.66	1

sequence), and the $v \sin i$ values are from the next section. Light curves are shown in Figure 4. The periods derived for AP 43 and AP 56 are certainly real, and the light curves are well defined. The photometric rotational velocities are consistent in all cases with the $v \sin i$ data. The periods, light curve shapes, and amplitudes are quite similar to those found for K stars in the Pleiades (van Leeuwen and Alphenaar 1982, hereafter VA). Van Leeuwen (1983) and SHSB have interpreted the Pleiades photometric variations as due to starspots, and we assume that the α Persei variables also have nonaxisymmetric spot distributions.

The data for AP 86 indicate that significant periodic behavior is present. However, aliasing problems prevent us from clearly distinguishing between the 4.17 hr and 5.06 hr periods.

IV. SPECTROSCOPY

We have obtained high-dispersion spectra of a large number of late-type dwarfs in the α Persei cluster in order to determine radial velocities (v_{rad}) and projected rotational velocities ($v \sin i$) for those stars. The spectra were secured with the echelle spectrographs of the 1.5 m telescope and the Multiple Mirror Telescope (MMT) on Mount Hopkins. Photon-

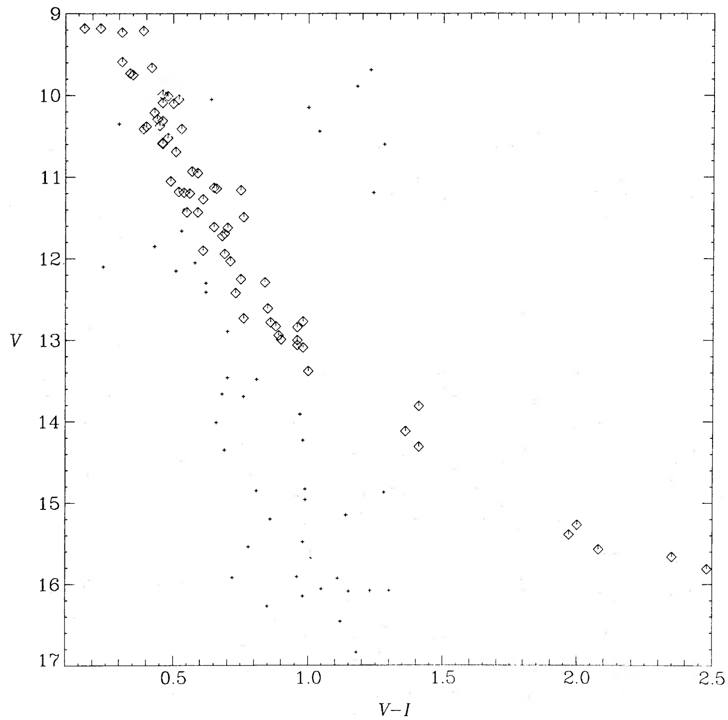

FIG. 2.—Color-magnitude diagram for the stars observed photoelectrically. Stars that are later identified as nonmembers are shown as small plus signs.

counting, intensified Reticon detectors were used at both telescopes (Latham 1982). These one-dimensional detectors record only one echelle order per exposure; typically, the 2048 pixels of the Reticon span about 50 Å. We chose two orders for all our observations, one centered on 5197 Å and a second centered on Hα. Spectra of two of the α Per stars observed at the 5197 Å order are shown in Figure 5. The absorption lines for the star in Figure 5*a* are not broadened beyond our instrumental resolution of 10 km s^{-1}.

Cross-correlation techniques (Tonry and Davis 1979) were used to derive radial and rotational velocities from the spectra. A detailed discussion of our methodology is given in SHSB. The instrumental resolution of the echelle spectrographs prevents us from deriving rotational velocity estimates for stars with $v \sin i < 10$ km s^{-1} given the signal-to-noise values in our spectra. Stars with $v \sin i > 80$ km s^{-1} for the 5197 Å order (50 km s^{-1} for the Hα order) have line profiles that are so broad and shallow that accurate radial and rotational velocities cannot be measured. Within that velocity range ($10 < v \sin i < 80$ km s^{-1}), comparison with published results for other late-type stars indicates that the rotational velocities are accurate to 10% with typical signal-to-noise spectra. Radial velocity measurements have accuracies ranging from 0.8 km s^{-1} for slowly rotating stars to 4 km s^{-1} for stars with $v \sin i > 70$ km s^{-1}.

The bright stars in the cluster were observed primarily at the 5197 Å order. As noted in § II, the faint end of our proper motion membership list was likely to contain a larger fraction of nonmembers than the bright end. By virtue of their faintness, those stars would also require the most observing time to

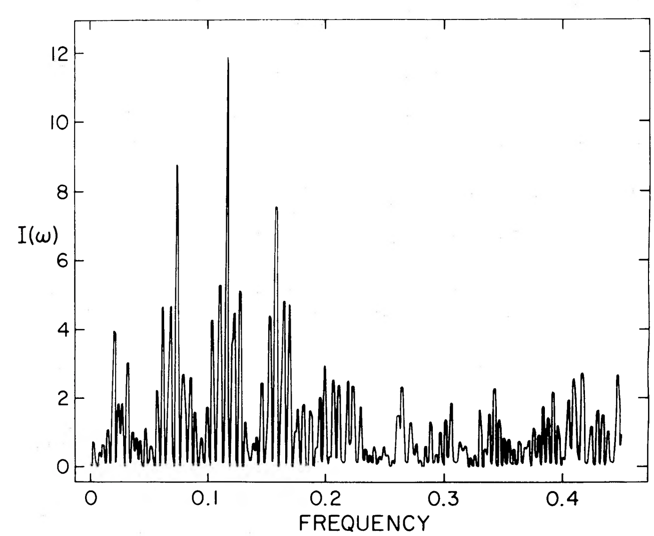

FIG. 3*a*

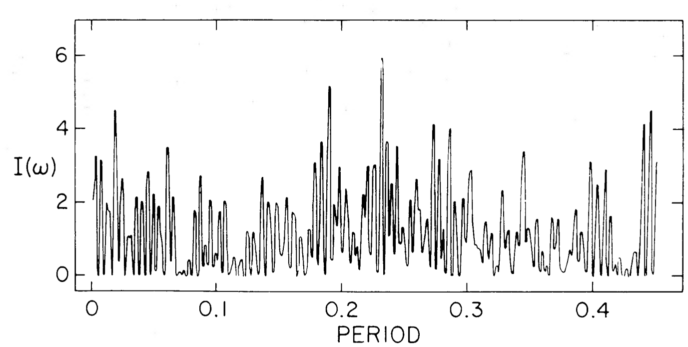

FIG. 3*b*

FIG. 3.—(*a*) Modified periodogram for the *V* band observations of AP 56. (*b*) Same as Fig. 3*a*, except after removal of the $P = 8.65$ hr periodicity.

TABLE 4

Photometry of Variables in Alpha Persei

JD 2,445,600.+	Phase	V	$B-V$	$V-R$	$R-I$
He 520					
67.6785	0.738	11.72	0.78	0.37	0.32
67.7271	0.818	11.68	0.79	0.37	0.31
67.7629	0.878	11.69	0.77	0.37	0.32
67.8014	0.942	11.67	0.78	0.36	0.32
67.8341	0.996	11.66	0.78	0.36	0.32
67.8653	0.048	11.66	0.78	0.35	0.31
67.8862	0.082	11.66	0.79	0.36	0.31
67.9264	0.149	11.68	0.79	0.37	0.31
68.6667	0.376	11.74	0.81	0.37	0.33
68.6903	0.416	11.75	0.81	0.38	0.33
68.8021	0.601	11.75	0.80	0.37	0.32
73.7638	0.830	11.66	0.80	0.36	0.33
73.8819	0.026	11.66	0.78	0.36	0.32
74.6146	0.241	11.69	0.79	0.36	0.33
74.7433	0.454	11.75	0.80	0.37	0.32
74.8688	0.663	11.70	0.79	0.37	0.33
75.6113	0.894	11.68	0.77	0.36	0.31
75.7457	0.116	11.67	0.77	0.36	0.32
75.8352	0.265	11.69	0.79	0.37	0.34
76.6336	0.589	11.71	0.79	0.38	0.33
76.7846	0.840	11.67	0.78	0.37	0.32
77.7775	0.486	11.74	0.81	0.37	0.32
78.5931	0.839	11.67	0.78	0.37	0.32
78.7321	0.069	11.66	0.78	0.37	0.32
78.8056	0.191	11.69	0.77	0.37	0.32
AP 15					
67.6737	0.764	14.12	1.30	0.78	0.56
67.7216	0.839	14.10	1.31	0.79	0.58
67.7567	0.893	14.10	1.29	0.79	0.56
67.7952	0.954	14.10	1.26	0.80	0.57
67.8285	0.006	14.10	1.28	0.78	0.58
67.8591	0.053	14.09	1.33	0.76	0.59
68.6556	0.298	14.11	1.29	0.79	0.57
68.6959	0.361	14.12	1.26	0.79	0.57
68.8070	0.534	14.18	1.29	0.78	0.58
73.7823	0.308	14.09	1.28	0.79	0.57
73.8966	0.486	14.13	1.30	0.78	0.59
74.6297	0.632	14.17	1.28	0.78	0.56
74.7523	0.823	14.11	1.29	0.76	0.58
75.6269	0.190	14.11	1.27	0.78	0.57
75.7566	0.392	14.09	1.29	0.76	0.58
75.8452	0.531	14.16	1.28	0.79	0.60
76.6443	0.780	14.12	1.28	0.78	0.58
76.8006	0.024	14.08	1.29	0.76	0.58
77.8323	0.636	14.17	1.28	0.79	0.58
78.6104	0.852	14.12	1.25	0.80	0.58
78.7434	0.059	14.07	1.30	0.74	0.58
AP 43					
67.6560	0.319	12.86	0.96	0.53	0.44
67.7091	0.413	12.86	0.97	0.53	0.45
67.7452	0.478	12.86	0.97	0.53	0.44
67.7848	0.548	12.85	0.96	0.52	0.45
67.8181	0.607	12.84	0.95	0.53	0.44
67.8501	0.664	12.84	0.97	0.53	0.44
68.6466	0.080	12.79	0.97	0.51	0.44
68.6855	0.149	12.81	0.98	0.52	0.44
68.7896	0.334	12.88	0.96	0.52	0.45
68.8334	0.412	12.88	0.97	0.52	0.44
68.8855	0.505	12.87	0.97	0.53	0.44
73.7733	0.198	12.81	0.97	0.52	0.44
73.8881	0.402	12.85	0.97	0.53	0.46
74.6220	0.707	12.85	0.98	0.52	0.43
74.7481	0.932	12.77	0.96	0.50	0.42
74.8754	0.158	12.81	0.97	0.51	0.46
75.6165	0.476	12.85	0.97	0.52	0.43
75.7522	0.717	12.85	0.96	0.53	0.45
75.8402	0.874	12.78	0.96	0.51	0.44
76.6390	0.294	12.84	0.98	0.53	0.44
76.7950	0.571	12.86	0.95	0.52	0.46
77.8288	0.410	12.86	0.97	0.54	0.45
78.5957	0.774	12.81	0.97	0.53	0.43
78.7343	0.021	12.77	0.95	0.51	0.43
AP 56					
67.7167	0.487	13.04	1.05	0.54	0.43
67.7507	0.582	13.03	1.01	0.54	0.43
67.7903	0.692	13.01	1.00	0.54	0.43
67.8237	0.784	12.97	1.02	0.53	0.43
67.8542	0.869	12.96	1.01	0.53	0.43
67.8813	0.944	12.93	1.02	0.52	0.42
67.9216	0.056	12.94	1.01	0.53	0.42
68.6612	0.108	12.96	0.99	0.53	0.43
68.7007	0.218	13.02	1.01	0.54	0.43
68.7174	0.264	13.03	1.01	0.55	0.43
68.8125	0.527	13.06	1.00	0.54	0.43
68.8806	0.717	13.01	1.00	0.53	0.43
73.7776	0.303	13.03	1.03	0.54	0.44
73.8901	0.615	13.01	1.01	0.54	0.44
74.6244	0.651	13.02	1.00	0.53	0.44
74.7499	0.999	12.91	1.01	0.49	0.43
74.8781	0.355	13.07	1.00	0.55	0.43
75.6188	0.411	13.07	1.01	0.55	0.43
75.6813	0.584	13.01	1.02	0.52	0.43
75.7539	0.785	12.97	1.00	0.53	0.44
75.8423	0.030	12.94	0.98	0.52	0.43
76.6417	0.249	12.99	1.02	0.53	0.44
76.7984	0.683	12.99	1.01	0.53	0.44
77.8303	0.545	13.03	1.02	0.53	0.44
78.5995	0.680	12.99	1.01	0.53	0.44
78.7362	0.059	12.91	0.98	0.52	0.42
78.8090	0.261	13.00	1.01	0.53	0.42
AP 70					
67.6445	0.6268	12.84	1.01	0.52	0.40
67.6646	0.6306	12.84	1.02	0.51	0.38
67.6889	0.6354	12.84	1.01	0.50	0.38
67.7320	0.6436	12.84	1.02	0.50	0.38
67.7688	0.6506	12.86	1.01	0.50	0.39
67.8070	0.6580	12.85	1.01	0.51	0.38
67.8396	0.6642	12.85	1.01	0.50	0.39
67.8702	0.6702	12.85	1.01	0.50	0.38
67.8910	0.6742	12.84	1.00	0.51	0.39
67.9112	0.6780	12.85	0.99	0.51	0.38
68.6362	0.8172	12.82	1.01	0.49	0.38
68.6743	0.8246	12.83	0.98	0.50	0.38
68.7063	0.8306	12.83	0.99	0.50	0.37
68.7618	0.8414	12.83	0.99	0.49	0.38
68.7757	0.8440	12.84	0.98	0.50	0.38
68.7966	0.8480	12.83	1.01	0.49	0.38
68.8223	0.8530	12.82	1.00	0.49	0.38
68.8709	0.8622	12.83	0.99	0.49	0.38
73.7603	0.8010	12.81	1.00	0.49	0.39
73.8783	0.8237	12.82	1.01	0.50	0.39
73.8992	0.8278	12.81	1.02	0.48	0.39
74.6119	0.9646	12.81	0.99	0.47	0.39
74.6611	0.9740	12.81	0.99	0.49	0.38
74.7414	0.9894	12.82	0.98	0.49	0.39
74.8032	0.0013	12.81	0.98	0.48	0.38
74.8660	0.0134	12.80	1.00	0.48	0.39
75.6091	0.1560	12.82	1.00	0.48	0.39
75.6541	0.1646	12.83	1.01	0.49	0.38
75.7440	0.1819	12.84	1.02	0.49	0.38
75.8329	0.1990	12.85	0.99	0.49	0.41
76.6315	0.3523	12.85	1.02	0.52	0.40
76.6779	0.3612	12.86	1.00	0.51	0.39

TABLE 4—*Continued*

JD 2,445,600.+	Phase	V	$B-V$	$V-R$	$R-I$
AP 70					
76.7726	0.3794	12.86	1.01	0.52	0.39
76.7904	0.3829	12.86	1.00	0.51	0.40
77.7758	0.5721	12.85	1.01	0.51	0.37
77.8345	0.5833	12.86	0.99	0.51	0.40
78.5901	0.7284	12.84	1.00	0.51	0.38
78.6149	0.7331	12.85	0.99	0.50	0.38
78.7295	0.7551	12.85	0.99	0.50	0.40
78.8040	0.7694	12.85	0.99	0.49	0.39
AP 86					
67.6514	0.845	14.27	1.34	0.80	0.61
67.7035	0.145	14.34	1.27	0.84	0.60
67.7389	0.349	14.37	1.30	0.85	0.60
67.7799	0.585	14.31	1.30	0.81	0.60
67.8119	0.770	14.30	1.31	0.81	0.61
67.8438	0.952	14.29	1.36	0.81	0.60
67.8751	0.132	14.28	1.31	0.81	0.59
67.9160	0.370	14.35	1.32	0.86	0.62
68.6417	0.550	14.33	1.30	0.84	0.60
68.6792	0.766	14.33	1.24	0.84	0.61
AP 86					
68.7105	0.946	14.29	1.34	0.81	0.59
68.7688	0.282	14.35	1.32	0.82	0.62
68.7813	0.354	14.37	1.35	0.83	0.58
68.8167	0.558	14.36	1.29	0.82	0.60
68.8757	0.899	14.30	1.36	0.80	0.61
68.8903	0.983	14.30	1.34	0.81	0.58
73.8859	0.771	14.29	1.35	0.80	0.59
74.6171	0.984	14.29	1.33	0.80	0.59
74.7458	0.724	14.33	1.31	0.80	0.64
74.8720	0.451	14.31	1.33	0.81	0.63
75.6139	0.727	14.30	1.33	0.79	0.60
75.6652	0.023	14.27	1.34	0.79	0.59
75.7489	0.505	14.34	1.31	0.81	0.62
75.8377	0.017	14.29	1.35	0.79	0.63
76.6365	0.619	14.30	1.30	0.83	0.60
76.7929	0.522	14.33	1.33	0.81	0.63
77.7804	0.212	14.32	1.30	0.82	0.59
77.8269	0.479	14.31	1.30	0.81	0.59
78.6053	0.964	14.27	1.31	0.81	0.61
78.7394	0.737	14.30	1.32	0.81	0.59
78.8118	0.155	14.30	1.34	0.81	0.60

obtain adequate spectra. Based on the Pleiades cluster results, we expected all faint (i.e., late type) members of the α Per cluster to have Hα strongly in emission. The most efficient way to identify cluster members at the faint end of our survey was therefore to obtain spectra centered at 6563 Å and to expose until Hα was clearly either in emission or in absorption. Those stars with Hα in absorption we identify as nonmembers, even though the spectra are generally too poor to obtain a reliable radial velocity. Those with Hα in emission are assumed to be members, and we have used the spectra to derive radial velocities and rotational velocities from fits to the emission-line profile (see SHSB). A spectrum of one of the late-type cluster members is shown in Figure 6.

Low-resolution (1.3 Å FWHM) spectra for about 30 of the cluster members have been obtained with the Cassegrain spectrograph of the MMT. Those spectra have been used to derive Ca II H and K emission strengths as a function of spectral type and rotational velocity (Hartmann *et al.* 1985). For those objects with $v \sin i > 60$ km s^{-1}, the low-dispersion spectra can be used to derive rotational velocity estimates via both cross-correlation analyses and Gaussian fits to the emission-line profiles.

The results of the spectroscopic survey are summarized in Table 6, which combines data from the different echelle orders, plus the low-dispersion spectra where appropriate.

TABLE 5

PERIODICITY DATA FOR ALPHA PERSEI STARS

Star	Period (hr)	False Alarm Probability	Rotation Velocity	$v \sin i$ (km s^{-1})
He 520	14.472	0.013	84	87
AP 15	15.361	0.033	57	52
AP 43	13.495	0.001	73	72
AP 56	8.651	0.0002	114	110
AP 70	123.5	0.003	8.2	<10
AP 86	4.165	0.004	207	140
AP 86	5.066	0.005	170	140

V. DISCUSSION

a) Cluster Membership and the H-R Diagram

The photometric and radial velocity data provide the best indicators of cluster membership for stars in our survey. Stars that fall more than 0.3 mag below or 1.2 mag above the apparent main-sequence locus are expected not to be members of the cluster (evolved stars excepted). Similarly, stars that have radial velocities significantly different from the cluster mean (and that are not spectroscopic binaries) are not likely to be members.

The radial velocity histogram depicted in Figure 7 shows an obvious narrow peak, corresponding to the cluster velocity, superposed on a smooth background of nonmembers. After eliminating certain nonmembers, we estimate that α Per members with $v \sin i < 20$ km s^{-1} exhibit a mean heliocentric radial velocity of -0.3 km s^{-1}, with a velocity dispersion of 1.3 km s^{-1}. This dispersion is only slightly larger than our expected errors, so that it represents an upper limit to the true velocity dispersion of the cluster. For stars with $v \sin i$ between 20 and 50 km s^{-1}, the mean heliocentric radial velocity is 1.5 km s^{-1}, and the dispersion is 2.3 km s^{-1}, while the rapid rotators exhibit a dispersion of about 4 km s^{-1}. The dispersions are consistent with our measurement errors.

We identify the probable cluster members as those stars with velocities within 3 km s^{-1} of the cluster mean for slow rotators ($v \sin i < 20$ km s^{-1}), and within 8 km s^{-1} of the mean for the rapid rotators. The Hα data provide another membership criterion for stars with $V > 13$ mag, as discussed previously. The individual membership criteria for each of the stars observed are listed in the fifth, sixth, and seventh columns of Table 6. In most cases, the three criteria agree; where they do not, the highest weight is given to the photometric criterion. Our final cluster membership estimates are given in the eighth column of Table 6.

A V versus $V-I$ diagram for just the probable and possible cluster members is shown in Figure 8. The zero-age main-sequence (ZAMS) line is the same as that used for the Pleiades papers (SHSB; Stauffer 1984), except that the assumed distance modulus and reddening to α Per are $(m-M)_0 = 6.1$ and

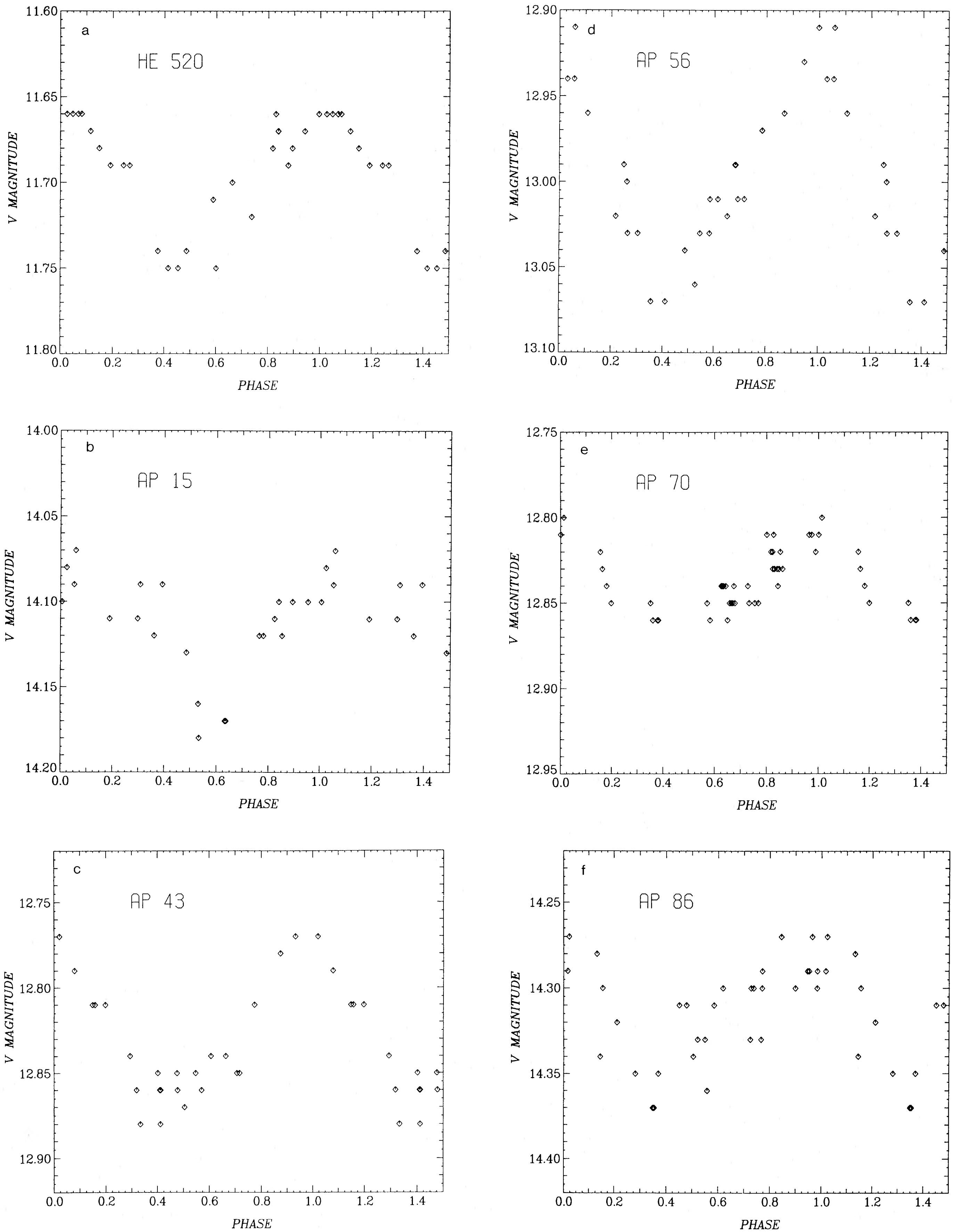

FIG. 4.—Proposed light curves for α Persei members observed more than 10 times. The ordinate axis range is 0.2 mag in all cases.

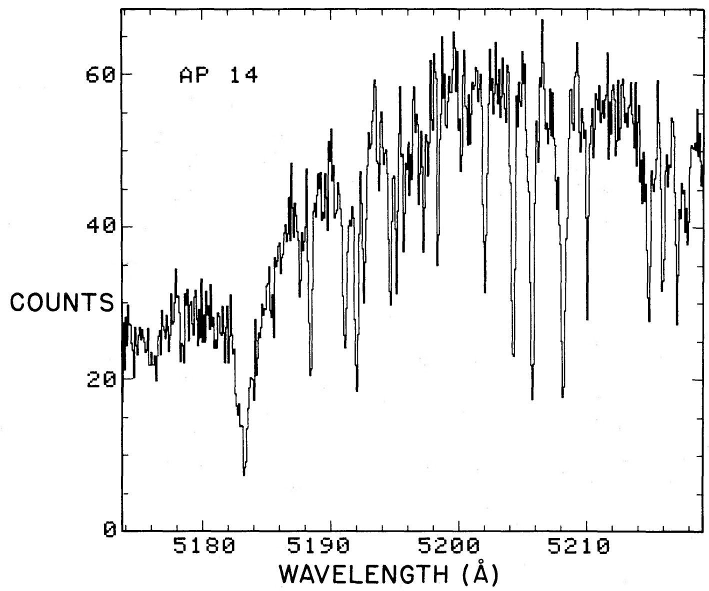

FIG. 5*a*

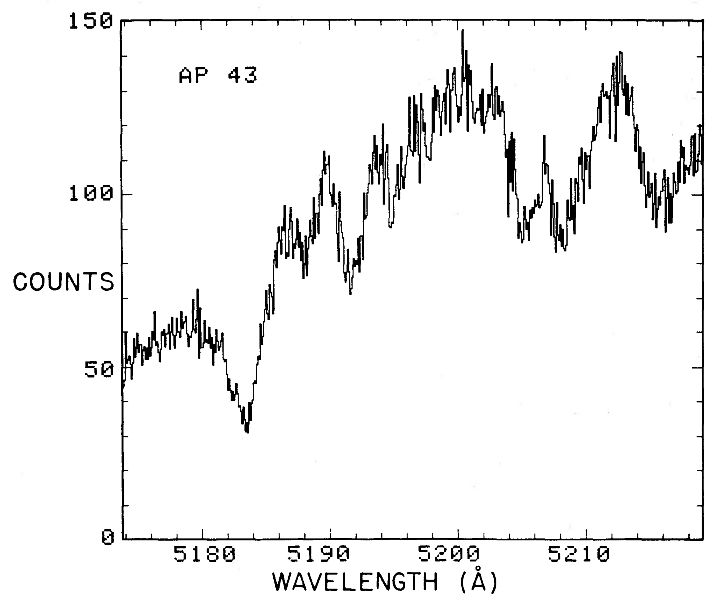

FIG. 5*b*

FIG. 5.—Spectra of two stars observed with the MMT echelle spectrograph. Based on our cross-correlation analysis, AP 14 has $v \sin i < 10$ km s^{-1}, while AP 43 has $v \sin i = 72$ km s^{-1}.

$E(V-I) = 0.16$. The upper portion of the α Per sample falls on the ZAMS to within the expected accuracy, while the stars fainter than $V = 13.5$ all lie above the ZAMS.

The position of the faint stars suggests that they are still contracting to the main sequence. However, there are potential problems with this interpretation. Preferential selection of binary cluster members in the proper motion survey in the appropriate magnitude range might produce the impression of pre–main-sequence stars (PMS). This effect could occur if the magnitude limit of our proper motion survey excluded our finding single cluster members in the color range $1.1 < V-I < 2.5$. The original identification of a PMS in the Pleiades (Landolt 1979; Stauffer 1980) was clouded by the near coincidence of the magnitude limit of Hertzsprung's (1947) proper motion survey and the proposed PMS turn-on point. We do not believe that our sample suffers from this problem. Since the stars in our survey were chosen from the R plate of the Palomar Sky Survey, our magnitude limit in an R versus $V-I$ plot would be a horizontal line. The same limit for a V versus $V-I$ plot should then be a line sloping slightly *downward* and to the right. Since the nonmembers of the cluster in Figure 2 extend to $V \approx 16.2$ at $V-I = 1.2$, we should not be strongly biased against single cluster members redward of $V-I = 1.2$ until $V > 16.2$. Thus we identify the stars fainter than $V \approx 13.5$ mag in Figure 8 as probable PMS stars. That identification should be viewed with some caution, however, until a more complete, somewhat fainter proper motion survey is obtained. It should also be clear that, with the small number of

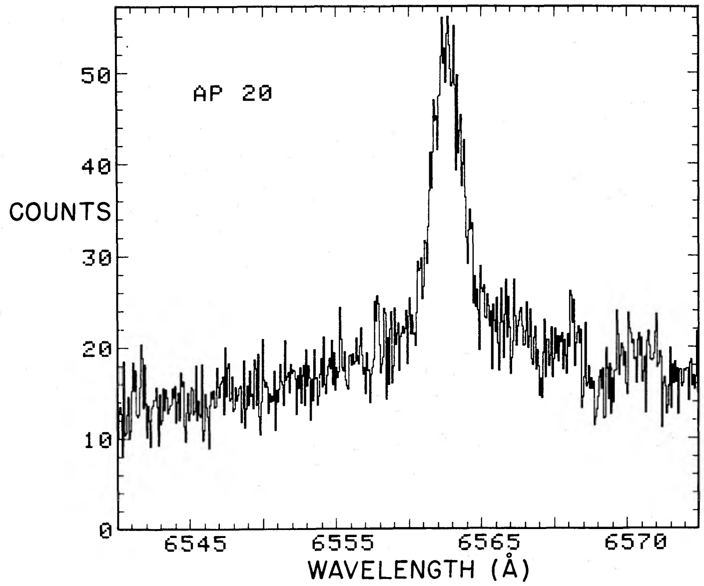

FIG. 6.—Echelle spectrum centered on Hα for AP 20

stars observed to date, we cannot identify the PMS turn-on point accurately, other than to say it is probably somewhere in the $13.5 < V < 15.5$ mag range.

VandenBerg *et al.* (1983) have calculated PMS isochrones for low-mass stars. Conveniently, one of the isochrones provided in their paper is for $\tau = 5 \times 10^7$ yr, the nominal age of the α Per cluster. We have transferred their isochrone from the theoretical log L versus log T_e diagram to our observational V versus $V-I$ diagram in the following manner. First, we examined Figure 2 of VandenBerg *et al.* to determine the displacement above the ZAMS as a function of temperature, $\Delta L(T)$, for the 5×10^7 yr isochrone. Temperatures were converted to $V-I$ via Veeder's (1974) relation between $T_{\rm eff}$ and Johnson $(R-I)$, the standard conversion between Johnson $(R-I)$ and Kron $(R-I)$, and a conversion between $(R-I)$ and $(V-I)$ derived from our own photometry. Finally, the bolometric corrections for the ZAMS and the PMS stars were assumed to be equal, thus allowing conversion of the $\Delta L(T)$'s to $\Delta V(V-I)$'s. The ΔV values were added to the observational ZAMS to produce the dashed isochrone shown in Figure 8. Because of the small number of stars in the proposed pre–main sequence and the possible problems caused by the magnitude cutoff of our proper motion survey, we caution against overinterpretation of the figure. However, the present observational data are consistent with the theoretical prediction.

b) *Evolution of Stellar Rotation*

The results summarized in Figure 7 demonstrate that the rapid rotators are associated with the cluster, and that the rapid rotation is not generally produced by tidal forces in close binary systems, since the orbital velocity variations would be much larger. Note that we have not included a few stars in Figure 7, such as AP 86, for which no accurate velocity can be measured, and AP 51, AP 56, and AP 79, which may be spectroscopic binaries.

Projected rotational velocities for the probable cluster members are indicated by the different symbol sizes in Figure 8. Stars for which no spectra have been obtained are shown as plus signs. Figure 8 appears to show little correlation between rapid rotation and spectral type—stars with $v \sin i > 25$ km s^{-1} occur among the G, K, and M dwarfs in α Per. That result differs from the Pleiades observations, in a manner

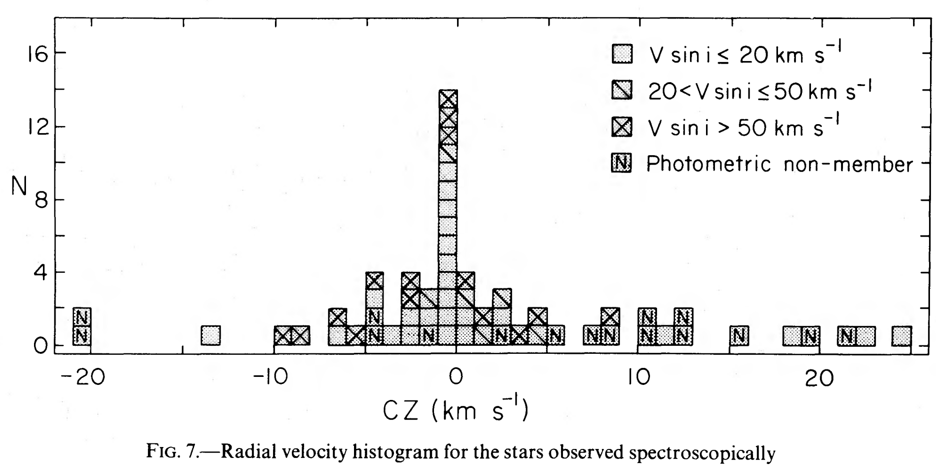

FIG. 7.—Radial velocity histogram for the stars observed spectroscopically

TABLE 6

SPECTROSCOPIC DATA

Star	$V-I$	Radial Velocity	Rotational Velocity	Membership			
				Phot.	*cz*	Hα	Final
He 326	0.51	0.2(3.6)	64.(10)	N	Y	...	N
He 330	1.18	−4.5(0.6)	<10	N	N	...	N
He 334	0.45	−2.1(1.2)	19(2)	Y	Y	...	Y
He 350	0.65	0.3(1.7)	47(4)	Y	Y	...	Y
He 407	0.52	−1.0(1.2)	28(2)	Y	Y	...	Y
He 444[a]	0.75	var	<10	Y	?	...	Y
He 453	0.53	−9.(2.5)	72(4)	Y	Y?	...	Y
He 457	0.68	−13.1(1.5)	19(2)	Y	N	...	Y
He 462	0.76	11.6(1)	<10	Y	N	...	Y
He 477	1.28	34.5(1)	<10	N	N	...	N
He 493	0.49	24.3(0.9)	<10	Y	N	...	Y
He 520	0.69	−6.0(6)	87(10)	Y	Y	...	Y
He 538	0.65	2.8(1.3)	11(3)	Y	Y	...	Y
He 600	0.61	−2.8(0.4)	11(2)	Y	Y	...	Y
He 601	0.59	−0.8(0.7)	15(1)	Y	Y	...	Y
He 660	0.50	2.4(1.6)	43(4)	Y	Y	...	Y
He 699	0.61	4.1(8)	90(15)	Y	Y	...	Y
He 707	0.64	10.2(1)	12(2)	N	N	...	N
He 709	0.59	3.5(5)	59(8)	Y	Y	...	Y
He 767	0.51	−1.2(0.8)	10(1)	Y	Y	...	Y
He 771	0.66	18.5(0.9)	11(1)	Y	N	...	Y
He 815	1.24	−20.2(1.5)	<10	N	N	...	N
He 841	0.44	1.7(3)	65(8)	Y	Y	...	Y
AP 1	1.28	8.7(0.8)	<10	N	N	N	N
AP 3	0.78	...	...	N	...	N	N
AP 4	1.15	...	...	N	...	N	N
AP 6	1.97	−4.(2)	<15	Y	N	...	Y
AP 7	1.05	25.5(1)	<10	N	N	...	N
AP 9	0.81	−20.3(0.9)	<10	N	N	...	N
AP 10	0.24	...	...	N	...	N	N
AP 14	0.69	−0.1(0.6)	<10	Y	Y	...	Y
AP 15	1.36	5.(3)	52(8)	Y	Y	Y	Y
AP 17	1.98	...	>60	Y	Y	...	Y
AP 19	0.70	−2.5(2)	61(5)	Y	Y	...	Y
AP 20	2.35	−8.5(5)	70(10)	Y	Y?	Y	Y
AP 21	2.08	1.5(1.6)	25(5)	Y	Y	...	Y
AP 25	0.75	−0.1(0.7)	12(2)	Y	Y	...	Y
AP 26	0.72	...	...	N	...	N	N
AP 28	0.97	−0.1(0.7)	12(1)	Y	Y	...	Y
AP 30	0.61	21.3(0.6)	<10	N	N	...	N
AP 31	0.69	−1.9(0.9)	<10	N	Y	...	N
AP 32	0.45	−1.5(4)	71(10)	Y	Y	...	Y
AP 33	0.89	0.5(0.7)	<10	Y	Y	...	Y
AP 36	0.97	10.1(0.6)	<10	N	N	...	N
AP 37	0.85	4.4(1)	29(2)	Y	Y	...	Y
AP 38	0.65	−0.4(1)	10(2)	Y	Y	...	Y
AP 41	0.71	0.6(0.5)	10(2)	Y	Y	...	Y
AP 43	0.96	−4.4(2.5)	72(4)	Y	Y	Y	Y
AP 45	0.86	−28.6(1.3)	<10	N	N	...	N
AP 46	0.62	7.6(0.7)	<10	N	N	...	N
AP 47	0.76	12.4(1)	<10	N	N	...	N
AP 51	0.46	var(?)	70(10)	Y	?	...	Y
AP 52	1.14	15.2(0.7)	<10	N	N	...	N
AP 54	0.70	−4.3(0.8)	<10	N	N	...	N
AP 55	0.97	2.1(0.6)	<10	N	Y	...	N
AP 56	0.96	−0.2(5)	110(30)	Y	Y	...	Y
AP 59	0.81	48(1)	<10	N	N	N	N
AP 60	2.47	−3.2(5)	105(10[b]	Y	Y	Y	Y
AP 61	0.98	62.4(0.7)	<10	Y	N	...	Y
AP 64	...	...	...	...	...	N	N
AP 65	0.91	−0.4(0.7)	10(1)	Y	Y	...	Y
AP 68	1.00	22.2(0.7)	<10	Y	N	...	Y
AP 70	0.88	−0.1(0.6)	<10	Y	Y	...	Y
AP 71	0.70	12.7(0.8)	<10	N	N	...	N
AP 72	0.87	−0.2(0.6)	<10	Y	Y	...	Y
AP 73	0.58	19.1(1.5)	<10	N	N	...	N
AP 75	1.42	−6.0(0.8)	11(1)	Y	N	Y	Y
AP 78	0.96	−0.1(0.6)	13(1)	Y	Y	...	Y
AP 79[c]	0.46	?	<20	Y	...	...	Y

TABLE 6—*Continued*

Star	$V-I$	Radial Velocity	Rotational Velocity	Membership			
				Phot.	*cz*	Hα	Final
AP 81	0.73	−35.6(0.7)	<10	Y	N	...	Y
AP 82	0.76	48.4(1)	<10	N	N	...	N
AP 85	1.30	...	...	N	...	N	N
AP 86	1.41	8.(9)	140(30)	Y	Y	Y	Y
AP 88	0.66	5.3(1.2)	15(2)	N	N	...	N

NOTE.—Numbers in parentheses are 1 sigma errors. Three ellipsis dots indicate that the quantity was not measured. The *cz* column indicates whether or not the star has a radial velocity consistent with cluster membership.

[a] SB1?

[b] The rotational velocity estimate is from a fit to the Hα profile.

[c] SB2?

that is consistent with the model outlined in SHSB, as discussed below.

The dependence of projected rotational velocity on color (spectral type) for the Pleiades and α Per stars is shown in Figure 9. For comparison, a similar diagram for field and Hyades stars is shown in Gray (1982). The Pleiades diagram includes data from SHSB and additional observations that will be reported in a separate paper (Stauffer, Hartmann, and Burnham 1985). The colors used here are intrinsic colors, with mean reddening corrections of $E(V-I) = 0.07$ and 0.16 mag for the Pleiades and α Per, respectively. The primary difference between either of the two young clusters and the field is the presence of the stars with $v \sin i > 25$ km s^{-1} for spectral types later than G2 in the young clusters. The Pleiades and α Per differ in that there are a number of rapid rotators among the G dwarfs in α Per, whereas stars of that spectral type in the Pleiades are all slow rotators.

Since low-mass T Tauri stars are generally slowly rotating (Vogel and Kuhi 1981), the late-type dwarfs in the α Per cluster, as well as similar stars in the older Pleiades cluster, must have spun up during contraction to the main sequence. SHSB assumed that the G dwarfs in the Pleiades were originally rapidly rotating but have spun down considerably upon arrival on the main sequence. The presence of rapid rotators among the G stars in α Per confirms this picture, since its upper main-sequence turnoff age of about 5×10^7 yr implies that 0.9 $M_\odot$ stars have only recently arrived on the main sequence, while stars of that mass in the Pleiades arrived on the main sequence 2×10^7 yr ago.

Endal and Sofia (1981) showed that by assuming a plausible

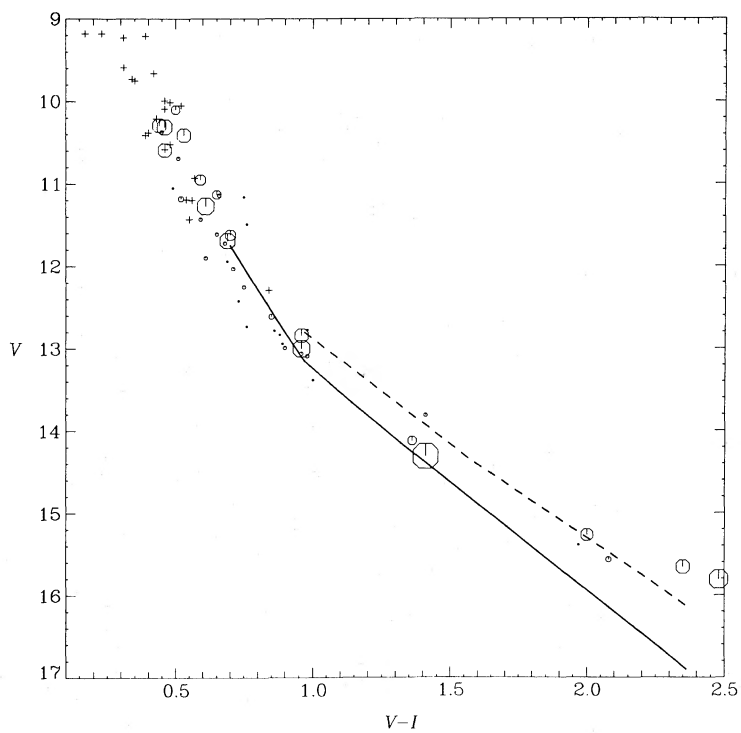

FIG. 8.—Color-magnitude diagram for stars believed to be members of the α Per cluster. The solid line is the ZAMS, shifted to the distance and reddening of the cluster. The dashed line shows the location of the 5×10^7 yr isochrone derived by VandenBerg *et al.* (1983). Stars with spectroscopic rotational velocity estimates are shown as octagons, with the size of the symbol proportional to the rotational velocity. Stars not observed spectroscopically are shown as plus signs.

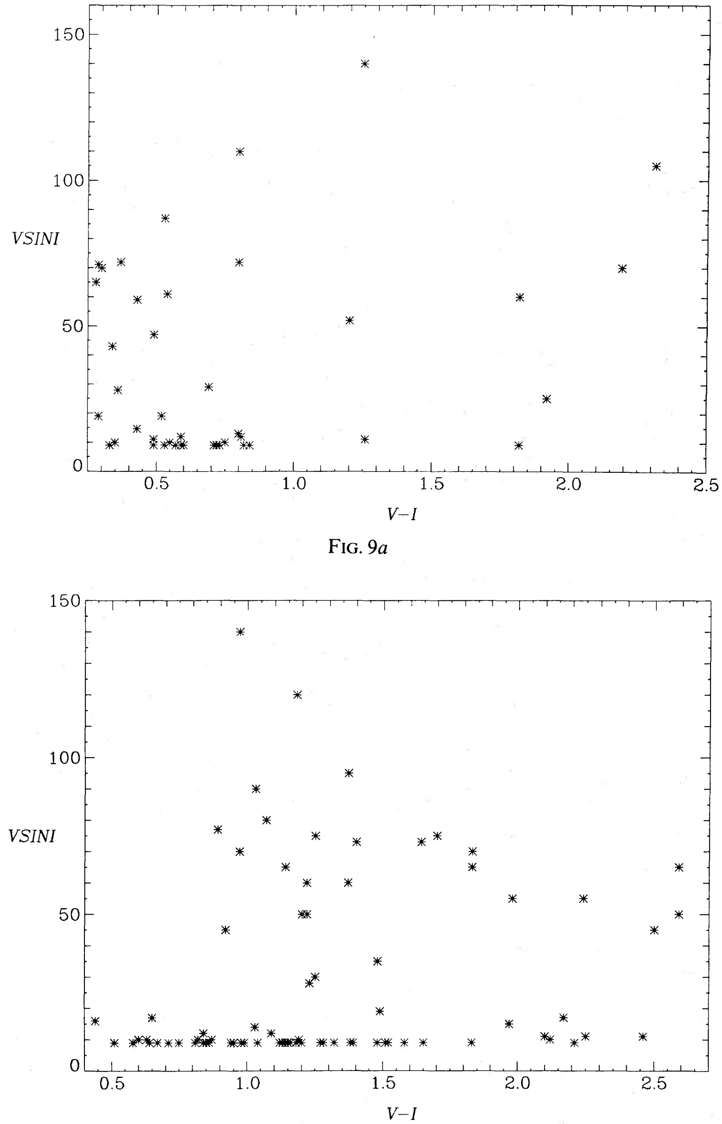

FIG. 9a

FIG. 9b

FIG. 9.—Projected rotational velocities for late-type stars in the (a) α Persei and (b) Pleiades clusters as a function of reddening-corrected $V-I$ color. Stars with $v \sin i$ upper limits of 10 km s^{-1} are shown at $v \sin i = 9$ km s^{-1}.

rate of angular momentum loss (Belcher and MacGregor 1976), G dwarfs can spin down from $v \sin i \approx 50$–100 km s^{-1} to $v \sin i \approx 10$ km s^{-1} over a time scale of a few $\times 10^7$ yr on the main sequence. According to their model calculations, only the outer convective envelope is affected initially by the wind, leaving the radiative core spinning rapidly. Since only a small fraction of the total moment of inertia of a 1 $M_\odot$ star is contained in the convective envelope, that facet of their model is an important contributor to the rapid spin-down. The presence of G star rapid rotators in α Per and their absence in the Pleiades indicate that real stars spin down at least as rapidly as predicted by Endal and Sofia. This suggests that some of the Pleiades G dwarfs have radiative cores spinning more rapidly than their convective envelopes.

As a final point, we note that the spread in $v \sin i$ at a given color shown in Figure 9 for the late-type stars in α Per and the Pleiades is probably due to a combination of causes. The possible contributors are the spread in initial angular momentum, the distribution of axial inclination angles, and the spread in age for low-mass stars in the two clusters. With the present relatively sparse data, it is not possible to separate those three contributors. We will eventually be able to estimate the sin i distribution by combining knowledge of the true rotational velocity, derived from the photometric periods, with the projected rotational velocities derived from the echelle spectra.

VI. SUMMARY

A new proper motion survey of faint stars toward α Persei has allowed us to select a list of possible low-mass members of the open cluster with which that star is associated. Optical photometry for those stars indicates that some are still contracting to the main sequence, with a PMS turn-on point in the range $13.5 < V < 15.5$. Several of the late-type stars are short-period, photometric variables with large rotational velocities and active chromospheres. The presence of such stars in another young cluster, the Pleiades, and their absence in the Hyades and the field indicate to us that this is an evolutionary effect. According to our model, the K dwarf stars in α Per should spin down to surface rotational velocities of less than 10 km s^{-1} within another few hundred million years, while the G dwarfs will spin down to similar velocities in 2–3 × 10^7 yr.

We will close with two small speculations. The first relates to the luminosity function of the α Per cluster. Figure 8 shows that we have found very few low-mass cluster members, compared with the number of high-mass members identified by HDK. In part, this is due to our having sampled only the inner 1.4 deg^2 of the cluster. However, after correcting for that difference, there is still a large deficiency of low-mass stars compared with a normal, field luminosity function. This may reflect either a general deficiency of low-mass stars in open clusters (van den Bergh and Sher 1960) or mass segregation (van Leeuwen 1980). We plan on doing a more complete proper motion study of the α Per cluster next season, after which we will be able to address this problem in more detail.

As the second speculation, we note that stars of approximately solar type in α Per have $10 < v \sin i < 100$ km s^{-1}. If that spread is primarily due to a spread in initial angular momentum, it indicates that the very early evolution of the proto–planetary nebulae around solar mass stars may be quite varied. A factor of 10 range in angular momentum of the proto–planetary nebulae would presumably result in a large variation in planetary semimajor axes and masses. It is interesting to speculate as to which end of the rotational velocity range characterized the early Sun.

We wish to thank D. R. Soderblom for useful discussions and a careful reading of the first draft of this paper. We also thank J. Peters and E. Horine for obtaining some of the spectra used in this study. This work was supported in part by the Scholarly Studies Program of the Smithsonian Institution.

REFERENCES

Abt, H. A., and Hunter, J. H. 1962, *Ap. J.*, **136**, 381.
Artyukhina, N. M. 1972, *Soviet Astr.—AJ*, **16**, 317.
Belcher, J. W., and MacGregor, K. B. 1976, *Ap. J.*, **210**, 498.
Crawford, D. L., and Barnes, J. V. 1974, *A.J.*, **79**, 687.
Endal, A. S., and Sofia, S. 1981, *Ap. J.*, **243**, 625.
Fresneau, A. 1980, *A.J.*, **85**, 66.
Gray, D. F. 1982, *Ap. J.*, **261**, 259.
Hartmann, L., Stauffer, J., Basri, G., and Kuhi, L. 1985, in preparation.
Heckmann, O., Dieckvoss, W., and Kox, H. 1956, *Astr. Nach.*, **283**, 109 (HDK).
Herbig, G. H., and Jones, B. F. 1981, *A.J.*, **86**, 1232.
Hertzsprung, E. 1947, *Ann. Leiden Obs.*, Vol. **19**, No. 1A.
Kraft, R. P. 1967*a*, *Ap. J.*, **148**, 129.
———. 1967*b*, in *Spectroscopic Astrophysics*, ed. G. Herbig (Berkeley: University of California Press), p. 385.
Landolt, A. 1979, *Ap. J.*, **231**, 468.
Latham, D. W. 1982, in *Instrumentation for Astronomy with Large Optical Telescopes*, ed. C. M. Humphries (Dordrecht: Reidel), p. 259.
Lockwood, G. W., Thompson, D. T., Radick, R. R., Osborn, W. H., Baggett, W. E., Duncan, D. K., and Hartmann, L. 1984, *Pub. A.S.P.*, submitted.
Mermilliod, J. C. 1981, *Astr. Ap.*, **97**, 235.
Mitchell, R. 1960, *Ap. J.*, **132**, 68.
Scargle, J. D. 1982, *Ap. J.*, **263**, 835.
Soderblom, D. R. 1983, *Ap. J. Suppl.*, **53**, 1.
Soderblom, D. R., Jones, B. F., and Walker, M. F. 1983, *Ap. J. (Letters)*, **274**, L37.
Stauffer, J. R. 1980, *A.J.*, **85**, 1341.
———. 1982, *A.J.*, **87**, 899.
Stauffer, J. R., Hartmann, L., and Burnham, N. 1985, in preparation.
Stauffer, J. R., Hartmann, L., Soderblom, D. R., and Burnham, N. 1984, *Ap. J.*, **280**, 202 (SHSB).
Tonry, J., and Davis, M. 1979, *A.J.*, **84**, 1511.
van Altena, W. F. 1974, *A.J.*, **79**, 826.
VandenBerg, D. A., Hartwick, F. D. A., Dawson, P., and Alexander, D. R. 1983, *Ap. J.*, **266**, 747.
van den Bergh, S., and Sher, D. 1960, *Pub. David Dunlap Obs.*, **2**, 203.
van Leeuwen, F. 1980, in *Star Clusters*, ed. James Hesser (Dordrecht: Reidel), p. 157.
———. 1983, Ph.D. thesis, State University of Leiden.
van Leeuwen, F., and Alphenaar, P. 1982, *ESO Messenger*, No. 28, p. 15 (VA).
Vaughan, A. H., Baliunas, S. L., Middelkoop, F., Hartmann, L. W., Mihalas, D., Noyes, R. W., and Preston, G. W. 1981, *Ap. J.*, **250**, 276.
Veeder, G. 1974, *A.J.*, **79**, 1056.
Vogel, S. N., and Kuhi, L. V. 1981, *Ap. J.*, **245**, 960.

J. NEAL BURNHAM and LEE W. HARTMANN: Harvard-Smithsonian Center for Astrophysics, 60 Garden St., Cambridge, MA 02138

BURTON F. JONES: Lick Observatory, University of California, Santa Cruz, CA 96064

JOHN R. STAUFFER: Dominion Astrophysical Observatory, 5071 W. Saanich Rd., Victoria, B.C. V8X 4M6, Canada